

# Improved theoretical calculations of InN in its $X^3\Sigma^-$ ground state and in the first $^3\Pi$ excited state

Lukáš Demovič<sup>a</sup>, Ivan Černušák<sup>a</sup>, Giannoula Theodorakopoulos<sup>b</sup>,  
Ioannis D. Petsalakis<sup>b</sup>, Miroslav Urban<sup>a,\*</sup>

<sup>a</sup> Department of Physical and Theoretical Chemistry, Faculty of Natural Sciences, Comenius University, Mlynská Dolina, SK-842 15 Bratislava, Slovakia

<sup>b</sup> Theoretical and Physical Chemistry Institute, The National Hellenic Research Foundation, 48 Vassileos Constantinou Avenue, Athens 116 35, Greece

Received 27 July 2007; in final form 12 September 2007

Available online 15 September 2007

## Abstract

Spectroscopic constants of the two lowest states of the InN molecule, the  $X^3\Sigma^-$  ground and the  $^3\Pi$  excited state were calculated using the restricted open-shell Hartree–Fock Coupled Cluster ROHF-CCSD(T) method with single, double and perturbative triples, the complete active space second-order perturbation theory (CASPT2) and the multireference configuration interaction (MRDCI) methods. Relativistic pseudopotentials (for MRDCI) and atomic natural orbital basis set for treating spin–orbit and scalar relativistic effects – ANO-RCC (for CCSD(T), CASPT2 and CASPT2/RASSI-SO) were used. The accuracy of different methods was compared correlating up to 26 valence and core-valence electrons of N and In atoms.

© 2007 Elsevier B.V. All rights reserved.

## 1. Introduction

The group-III nitrides (MeN) are interesting due to their applications ranging from solar cells to optoelectronic devices [1]. The results of various experiments and modeling showed that MeN alloys can emit light from the near infrared (prevailing InN) to the near ultraviolet (prevailing GaN) [2]. Interestingly, in 1997 Ponce and Bour [3] stated that:

With the advent of the nitride-based semiconductors, the long search for bright solid-state sources covering the full range of the visible spectrum seems to be over.

Yet, it was just a starting point in the subsequent story. Focal property of In and Ga nitrides is their band-gap that, according to the way the ternary alloy is prepared, can vary from 0.7 eV (molecular-beam epitaxy films [2,4]) to 2.1 eV

(sputtered films [5]). The band gap of 0.7 eV can be attributed to wurtzite structure, whereas the larger one is typical for polycrystalline phase from sputtered films.

For a better understanding of the processes underlying technological applications of MeN species it is important to know spectroscopic constants and electric properties of participating diatomics in the ground and low-lying excited states [6–8]. However, the amount of systematically obtained accurate experimental or theoretical data is rather limited. Most of the theoretical studies on InN were limited to density functional theory (DFT) band-structure calculations [9–11] and MeN clusters [12,13]. None of these studies reported potential energy curves and molecular data on diatomic InN in the ground and excited states. Only in a recent MRDCI study such calculations were performed on InN by two of the present authors [8].

In MRCI the authors try to calculate typically up to 16–18 spectroscopic states on MeN diatomics relying on the multireference treatment. The advantage of the MRDCI method [14], used in this work, is the significant reduction of the CI space due to sophisticated, energy threshold based configuration selection, while the reference

\* Corresponding author. Fax: +421 2 65429 064.

E-mail address: [urban@fns.uniba.sk](mailto:urban@fns.uniba.sk) (M. Urban).

space is determined using preliminary calculations over the required geometries. The previous MRDCI calculation [8], being the first ab initio calculation on InN, aimed at the investigation of 17 excited states, with equal accuracy, without exhausting the possibilities for improving the calculational procedure. As a result, it was not possible to calculate accurately the energy difference between the  $X^3\Sigma^-$  and  $^3\Pi$  states. Previous MRDCI study lead to very small  $T_e$  (0.04 eV) [8].

Our approach in the present paper is different. Instead of calculating a variety of low-lying excited states we pay an attention just to the  $X^3\Sigma^-$  ground and the  $^3\Pi$  excited states with the aim to calculate reliably their molecular properties. We note that for selected states, not affected by quasidegeneracy, the CCSD(T) method is more straightforward to use and is normally more reliable than other highly correlated wave function methods with comparable computational effort. When all singly and doubly excited states are considered in MRCI with respect to the CASSCF wave function the number of explicitly correlated electrons in the CI step must be limited to keep calculations computationally feasible. It is practical to explicitly correlate 8 valence electrons only, i.e.,  $ns^2np^1$  electrons of the group-III metal element and  $2s^22p^3$  electrons of nitrogen. Such approach has been used in the previous paper [8]. Denis and Balasubramanian [7] have shown that after including in CCSD(T) also core-valence  $3p^63d^{10}$  electrons of Ga in the GaN molecule the  $X^3\Sigma^- \rightarrow ^3\Pi$  excitation energy is reduced by more than by 50%. The equilibrium bond length is lowered by 0.05–0.06 Å for both states when going from 8 to 18 correlated electrons. Their MRCI calculations for the ground state show that  $\omega_e$  increased by only  $13\text{ cm}^{-1}$  and the dipole moment increased by 0.16 Debye after including the  $3d^{10}$  electrons. No information about the importance of correlating the  $3d^{10}$  electrons is given for  $\omega_e$  at the CCSD(T) level. Thus, it is necessary to correlate at least 18 electrons, even if this is not documented in a systematic way. It is interesting to note that even with 8 correlated electrons only, the  $X^3\Sigma^-$  state of GaN is correctly calculated [7] as the ground state by CCSD(T), while for valence isoelectronic BN and AlN molecules [15–17] the authors [17] report some problems of CCSD(T) in the proper ordering of different states. We believe that systematic consideration of the number of explicitly correlated electrons within MRDCI, CASPT2, and CCSD(T) methods, using InN as a typical example of the group-III nitrides may bring some methodological knowledge useful in subsequent theoretical treatment of larger clusters of these molecules potentially important from the technological point of view. Finally, we also present results with two differently constructed pseudopotentials in which  $5s^25p^1$  or  $4d^{10}5s^25p^1$  subshells are included in the reference valence set from which SCF orbitals are created.

Even if indium is not too heavy element, spin–orbit effects may affect spectroscopic properties of the two states under consideration differently. This follows from the fact

that the spin–orbit splitting of the  $^3\Pi$  state may be large enough to push one of the SO split components of InN closer towards (even if not below) the  $^3\Sigma^-$  state. Related calculations were recently published for the indium fluoride molecule [18]. A possibility of the reversed sequence of the  $^3\Sigma^-$  and the  $^3\Pi$  states due to spin–orbit effects is quite expected for the heaviest molecule in the MeN series, TIN, which will be treated in a separate paper.

## 2. Calculations

All calculations were performed within the  $C_{2v}$  symmetry, the  $z$ -axis coinciding with the In–N bond. In MRDCI calculations, relativistic effective core potential (RECP) have been employed for the inner shells, leaving 4d, 5s, and 5p subshells for indium [19] and 2s and 2p for nitrogen [20] in the valence space. More specifically, when using RECPs we performed 18 electron SCF and either 8 or 18 electron MRDCI calculations. In all cases we include the FCI correction. In all-electron CC and CASSCF/CASPT2 calculations we used ANO-RCC basis set [21] with large contractions for both indium ( $22s19p13d5f3g$ )/[ $10s9p8d5f3g$ ] and nitrogen ( $14s9p4d3f2g$ )/[ $8s7p4d3f2g$ ]. The number of correlated electrons (8, 18 and 26, i.e.  $2s^22p^3$  electrons for N and  $5s^25p^1;4d^{10}5s^25p^1$ ; and  $4s^24p^64d^{10}5s^25p^1$ , respectively, for In) in CC and CASPT2 calculations was systematically increased to elucidate the core-valence effects.

In spin-free calculations, we used two valence active spaces in the CASSCF step. Space I included 8 electrons in 8 orbitals ( $12a_1/5b_1/5b_2/2a_2$  inactive,  $4a_1/2b_1/2b_2/0$  active), followed by CASPT2 calculations with 8, 18 and 26, respectively, correlated electrons. Space II included 8 electrons in 14 orbitals ( $12a_1/5b_1/5b_2/2a_2$  inactive,  $7a_1/3b_1/3b_2/1a_2$  active), followed by CASPT2 with 18 correlated electrons only.

Relativistic effects in MRDCI were included in the RECPs developed for indium and nitrogen [19,20]. The second order spin-free Douglas–Kroll–Hess Hamiltonian (DKH) [22] was used to calculate molecular properties considering scalar relativistic effects within the spin-adapted CCSD(T) [23,24] and the CASPT2 method [25] as implemented in the MOLCAS program [26]. This should be considered as a lowest order counterpart of the spin-free infinite-order two-component method [27], to take into account both scalar and spin–orbit one-electron relativistic effects simultaneously. We note that the DKH method usually provides reasonably accurate account of the scalar relativistic effects. CCSD and CCSD(T) dipole moments and dipole polarizabilities were calculated using the finite field perturbation theory [28] with external electric field strengths 0.0005, 0.001, and 0.002 a.u., respectively.

Spin–orbit effects are expected to be important particularly for the  $^3\Pi$  excited state of InN. We exploited the Restricted Active Space State Interaction method, CASSCF/CASPT2/RASSI-SO (shortly CASPT2/RASSI-SO) introduced by Roos and Malmqvist [29]. The performance

of this method and comparison with experiment were clearly demonstrated in the cited paper. Our calculations were performed using both active spaces (I and II), with 18 electrons correlated in the CASPT2 step. Four states ( $^3\Pi$ ,  $^3\Sigma^-$ ,  $^5\Pi$ , and  $^5\Sigma^-$ ) dissociating to the atomic ground states ( $^4S\text{ N}$ ,  $^2P\text{ In}$ ) were considered, leading to 24 relativistic states.

### 3. Results and discussion

#### 3.1. Spin-free calculations

CASPT2 and MRDCI potential energy curves are shown in Fig. 1. Obviously, correlating the  $4d^{10}$  electrons is important particularly for the  $^3\Pi$  state. For example, when correlating also  $4d^{10}$  electrons in the MRDCI calculations the gap between the  $^3\Pi$  and the  $X^3\Sigma^-$  states, excitation energy  $T_e$ , decreases significantly.

Using the CASPT2 method, we have examined further extension of the correlation space by including also  $4s^2 4p^6$  electrons (see upper part of Fig. 1). This alters the shape of the potential energy curves of both states marginally.

Systematic comparison of spectroscopic constants using MRDCI, CASPT2, and CCSD(T) methods is in Table 1. The first row reproduces our previous results employing RECP with only the  $5s$  and  $5p$  subshells in the valence space for In and  $2s$  and  $2p$  subshells for N (i.e., 8 electrons used in SCF). Results with RECPs in which  $4d$  electrons along with  $5s$  and  $5p$  subshells are left in the valence space of In are in the second row of Table 1. The comparison clearly demonstrates large sensitivity of spectroscopic constants to the selection of the core potential. Most affected is the  $^3\Sigma^- \rightarrow ^3\Pi$  excitation energy, by 0.275 eV. With the RECP leaving 18 electrons in the valence space and correlating 8 electrons in MRDCI,  $T_e$  is too large, 0.315 eV.

Correlating 18 electrons,  $T_e$  goes down to 0.12 eV, which agrees reasonably well with best results from CASPT2 and CCSD(T).

CCSD(T) results for  $T_e$  exhibit similar trends as MRDCI with respect to correlating 8 or 18 electrons ( $T_e = 0.293$  and  $0.191$  eV, respectively). The sensitivity of CCSD(T) results to the number of correlated electrons is also reflected in relatively large contributions to  $T_e$  arising from the triple excitations in CCSD(T), see Table 1. Final extension to 26 correlated electrons modifies  $T_e$  marginally ( $T_e = 0.189$  eV). CASPT2 excitation energy (smaller active space I) is much less sensitive to the number of correlated electrons than it was with CCSD(T), but the trend is analogous. With the active space II and correlating 18 electrons,  $T_e$  is almost the same as with the smaller active space I. Best values of  $T_e$  calculated with our three methods lie in the interval of 0.11–0.19 eV.

The pattern with respect to the number of electrons correlated in MRDCI, CASPT2 and CCSD(T) is qualitatively the same for  $R_e$  and  $T_e$  with all three methods. We note that after increasing the number of correlated electrons from 8 to 18 is  $R_e$  of the  $X^3\Sigma^-$  state reduced by 0.246 a.u. when using CCSD(T) and by 0.046 a.u. with CASPT2.  $R_e$  of the  $^3\Pi$  state is reduced with the two methods by 0.283 and 0.048 a.u., respectively. Less transparent pattern is found for  $\omega_e$  of the ground  $X^3\Sigma^-$  state which is largest with 8 electrons correlated in CCSD(T) and decreases by  $43\text{ cm}^{-1}$  when correlating 18 and 26 electrons, in contrast to MRDCI which exhibit the opposite tendency.  $\omega_e$  of the  $X^3\Sigma^-$  state calculated with CASPT2 is more sensitive to the selection of the active space than to the number of correlated electrons. The same holds for the  $^3\Pi$  state. In addition, we see no regular trend of  $\omega_e$  for this state with increasing number of correlated electrons in CASPT2. Differences in spectroscopic constants are understandable considering the different mechanism of

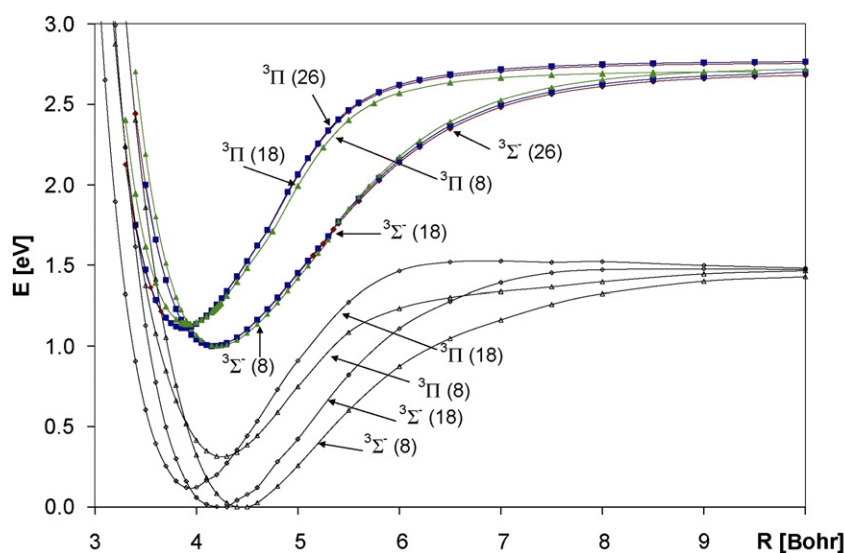


Fig. 1. CASPT2 (active space I) and MRDCI potential energy curves of InN. Numbers in parentheses refer to the number of correlated electrons. Lower group of curves result from the MRDCI data, upper curves arise from CASPT2 (shifted by 1 eV up for better readability).

Table 1  
Spectroscopic properties of non-relativistic triplet states of indium nitride

State method	Electrons correlated	$X^3\Sigma^-$		$1^3\Pi$		$T_e$ (eV)
		$R_e$ (bohr)	$\omega_e$ (cm $^{-1}$ )	$R_e$ (bohr)	$\omega_e$ (cm $^{-1}$ )	
Previous work <sup>a</sup>	8	4.044	486.4	3.761	563.0	0.040
MRDCI/RECP	8	4.451	426.1	4.428	441.4	0.315
MRDCI/RECP	18	4.259	537.0	3.952	632.4	0.119
CASPT2/ANO-RCC <sup>b</sup>	8	4.215	439.0	3.921	527.6	0.137
Ditto with averaged $\pi$ -orbitals				3.933	524.1	0.126
CASPT2/ANO-RCC <sup>b</sup>	18	4.169	439.1	3.873	536.5	0.112
Ditto with averaged $\pi$ -orbitals				3.875	533.7	0.116
CASPT2/ANO-RCC <sup>b</sup>	26	4.171	436.6	3.871	534.8	0.108
Ditto with averaged $\pi$ -orbitals				3.873	532.1	0.111
CASPT2/ANO-RCC <sup>c</sup>	18	4.163	447.3	3.884	522.3	0.111
CCSD(T)/ANO-RCC	8	4.417	488.5	4.185	512.5	0.293 (0.370) <sup>d</sup>
CCSD(T)/ANO-RCC	18	4.171	445.1	3.902	516.1	0.191 (0.282) <sup>d</sup>
CCSD(T)/ANO-RCC	26	4.169	445.5	3.900	517.4	0.189 (0.280) <sup>d</sup>

<sup>a</sup> Ref. [8].

<sup>b</sup> Active space I.

<sup>c</sup> Active space II.

<sup>d</sup> CCSD results in parentheses.

treating the dynamic correlation within the three methods. Nevertheless, our best results for  $\omega_e$  with CCSD(T) and CASPT2 (18 electrons correlated, active space II) lie in quite narrow interval, 445–447 cm $^{-1}$  for the  $X^3\Sigma^-$  state and 517–522 cm $^{-1}$  for the  $1^3\Pi$  state. MRDCI results for  $\omega_e$  are too large. We remind that in MRDCI we used a significantly smaller basis set [19] than in CASPT2 and CCSD(T) calculation.

Table 1 contains two sets of CASPT2 data for the  $1^3\Pi$  state: with and without averaging the  $\pi$ -orbitals. Non-averaged orbitals represent a symmetry broken solution resulting from a particular selection of reference orbitals in the computational  $C_{2v}$  symmetry. Fortunately  $R_e$ ,  $\omega_e$  and  $T_e$  with the averaged and non-averaged  $\pi$ -orbitals are generally similar. Also single-determinant ROHF CC results may be affected by the selection of the symmetry broken reference orbitals. Averaging could be done by reducing the symmetry to  $C_2$ , which brought some computational problems. It is encouraging that the CCSD(T) results (18 and 26 correlated electrons) agree reasonably well with the cluster of CASPT2 data.

### 3.2. Spin-orbit calculations

Six different relativistic states arise from the  $1^3\Pi$  and  $3^3\Sigma^-$  states of InN: 2, 1,  $0^+$  and  $0^-$  (corresponding to  $1^3\Pi$ ) and 1,  $0^+$  ( $3^3\Sigma^-$ ). For comparison, we present in Table 2 the results obtained in both active spaces. The choice of the active space in spin-orbit calculations modifies the location of the avoided crossing leading to non-negligible differences in  $\omega_e$  and  $T_e$  for the states 1 and  $0^+$ .

As one can see from Table 2 and Fig. 2, the relativistic ground state of the InN molecule is  $0^+$  (with almost the same  $R_e$  and  $\omega_e$  as for the spin-free ground state  $3^3\Sigma^-$ ). Two avoided crossings, corresponding to 1 and  $0^+$  states, can be seen in Fig. 2. Without these crossings the spin-

Table 2

Spectroscopic properties of the relativistic states of indium nitride. CASPT2/RASSI-SO/ANO-RCC calculations<sup>a,b</sup>

State	$R_e$ (bohr)	$\omega_e$ (cm $^{-1}$ )	$T_e$ (eV)	$D_e$ (eV)
$X^3\Sigma^-$ <sup>c</sup>	4.163 (4.169)	447.3 (439.1)	–	1.68 (1.77) <sup>d</sup>
$1^3\Pi$ <sup>c</sup>	3.884 (3.873)	522.3 (536.5)	0.111 (0.112)	1.57 (1.65) <sup>c</sup>
$0^+$	4.157 (4.163)	441.1 (433.1)	–	1.54 (1.63)
1	4.157 (4.166)	441.6 (439.2)	0.001 (0.001)	1.54 (1.63)
2	3.882 (3.869)	522.6 (538.2)	0.100 (0.099)	1.44 (1.53)
$0^-$	3.887 (3.876)	521.6 (535.6)	0.133 (0.138)	1.41 (1.49)
1	3.940 (3.936)	789.4 (718.3)	0.133 (0.139)	1.41 (1.49)
$0^+$	3.942 (3.937)	705.6 (719.2)	0.154 (0.163)	1.60 (1.66)

<sup>a</sup> Inactive orbitals  $12a_1/5b_1/5b_2/2a_2$ , active orbitals  $7a_1/3b_1/3b_2/1a_2$ , 18 correlated electrons in CASPT2.

<sup>b</sup> Data in parentheses refer to active orbitals  $4a_1/2b_1/2b_2/0a_2$ .

<sup>c</sup> Spin-free results.

<sup>d</sup>  $D_e$  from CCSD(T) with 26 correlated electrons is 1.765 eV.

<sup>e</sup>  $D_e$  from CCSD(T) with 26 correlated electrons is 1.576 eV.

orbit effects on the InN molecule would be negligible. Instead, three pairs of similar states are produced. The first pair includes two lowest states  $0^+$  and 1, with the spectroscopic properties very close to the spin-free  $3^3\Sigma^-$  state. The second pair (2,  $0^-$ ) is the only one which is not affected by the avoided crossings, leading to similar  $R_e$  and  $\omega_e$  as in the first excited spin-free  $1^3\Pi$  state. Moreover, average excitation energy of these states is not far from  $T_e$  of the spin-free  $1^3\Pi$ . The third pair includes second 1 and  $0^+$  states, which are most affected by spin-orbit effects. Bond lengths of these states are closer to the  $1^3\Pi$  state than to the  $3^3\Sigma^-$  state, but the respective harmonic frequencies  $\omega_e$  are higher by 220–330 cm $^{-1}$  when compared to both spin-free low-lying states. This feature can be clearly seen in Fig. 2 – avoided crossings of  $0^+$  and 1 states lead to narrower potential energy curves.

Dissociation energies of all relativistic states are mainly affected by the relatively large spin-orbit splitting of the

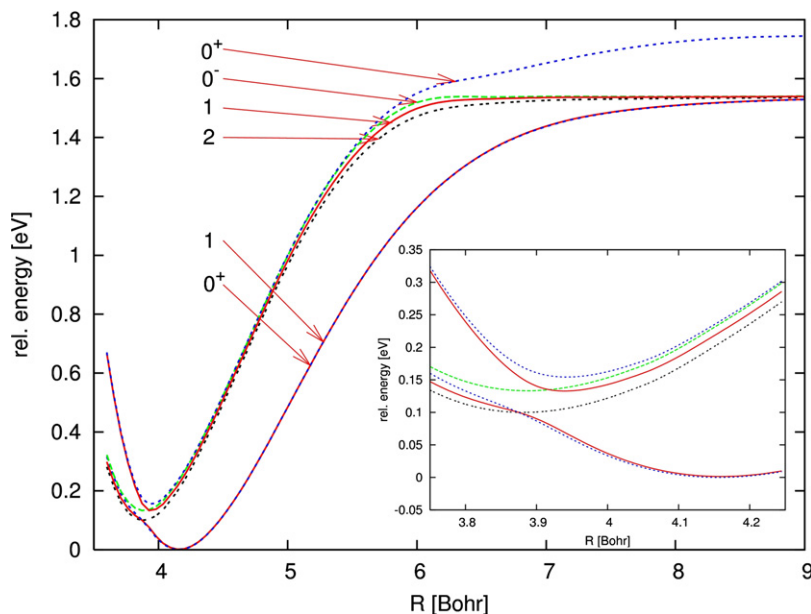


Fig. 2. CASPT2/RASSI-SO (active space II) potential energy curves of six lowest relativistic states. Inset shows detail around the avoided crossing region and the minima.

(2 + 4)  $^2\text{P}$  states of In (experimental value is 0.276 eV [29]). Twenty-four relativistic states of InN, including degeneracies, which arise from four spin-free states ( $^3\Pi$ ,  $^3\Sigma^-$ ,  $^5\Pi$ ,  $^5\Sigma^-$ ) dissociating to the ground atomic states ( $^4\text{S}$  of nitrogen and  $^2\text{P}$  of indium) are divided in the dissociation limit into 8 and 16 states with the energy gap of  $\sim 0.25$  eV. This value agrees reasonably well with the experimental SO splitting of the  $^2\text{P}$  states of In. This behavior is expected, since the splitting of the  $^4\text{S}$  state of N is negligible. As one can see from Fig. 2, the only state out of the nine lowest states not belonging to the lower group is  $0^+$ , whose dissociation energy is thus the highest of all the states considered. For all other states the differences in  $D_e$  due to the SO splitting (not larger than 0.03 eV in the larger active space, see Table 2) can be attributed to the SO splitting in the equilibrium region.

### 3.3. Dipole moments and dipole polarizabilities

Since the pattern of changes of spectroscopic constants with the number of correlated electrons is similar for all

Table 3

Dipole moments (Debye) and parallel polarizabilities (a.u.) of InN (ANO-RCC basis set,  $R_e$  taken from the last row of Table 1)

Method	Electrons correlated	$^3\Sigma^-$		$^3\Pi$	
		$\mu$	$\alpha_{\parallel}$	$\mu$	$\alpha_{\parallel}$
HF		2.988	58.69	2.669	65.61
CCSD	8	2.828	65.88	2.075	62.93
CCSD	18	3.412	65.78	2.693	69.09
CCSD	26	3.419	65.56	2.709	68.96
CCSD(T)	8	2.725	68.96	1.959	64.55
CCSD(T)	18	3.324	69.06	2.602	71.18
CCSD(T)	26	3.325	68.87	2.612	71.06

three correlated methods only results for dipole moments and dipole polarizabilities calculated with CCSD and CCSD(T) methods are presented in Table 3. To correlate just 8 valence electrons of InN is insufficient for both states. At the same time, to correlate 26 valence and core-valence electrons is not needed for dipole moments of both  $X^3\Sigma^-$  and  $^3\Pi$  states. The electron correlation effect is larger for the dipole moment and the parallel polarizability of the ground  $X^3\Sigma^-$  state (representing 10% and 14.8% of the final value, respectively) than for the  $^3\Pi$  state (2% and 7.7%, respectively).

## 4. Conclusions

We have demonstrated the performance of the spin-free CCSD(T) and CASPT2 methods in obtaining the bond length and the vibrational harmonic frequency for both low-lying  $X^3\Sigma^-$  and  $^3\Pi$  states of the InN molecule. Recommended  $R_e$  for the  $X^3\Sigma^-$  and the  $^3\Pi$  states are 4.17 and 3.90 bohr, harmonic frequencies are 445 and 517  $\text{cm}^{-1}$ , respectively. Results using MRDCI with effective core potentials and CASPT2 results deviate slightly from these values. For obtaining reasonable results, at least 18 electrons must be considered in the treatment of the dynamic electron correlation. The excitation energy varies slightly with the method, lying in the interval of 0.11–0.19 eV. The highest value follows from CCSD(T). Since the largest  $t_1$  and  $t_2$  CCSD amplitudes near the equilibrium distance are reasonably low, 0.03 ( $t_1$ ) and 0.03 ( $t_2$ ) for the  $X^3\Sigma^-$  state and are still acceptable for the  $^3\Pi$  state (0.14 ( $t_1$ ) and 0.05 ( $t_2$ ), respectively), we expect that CCSD(T) should be highly reliable in predicting molecular properties of InN. Good performance of the single-determinant reference CCSD(T) method is also supported by CI calculations

which show that the leading CI configuration is larger than 0.9 for both  $^3\Sigma^-$  and the  $^3\Pi$  states, in line with previous findings for the isoelectronic GaN molecule [7].

Spin-orbit interactions lead to the avoided crossing of the 1 and  $0^+$  states resulting in non-negligible change in the shape of the potential energy curves. Thus, spectroscopic properties of InN are slightly modified.  $R_e$  and  $\omega_e$  for the ground  $0^+$  state are lower by 0.006 a.u. and  $6\text{ cm}^{-1}$ , respectively, than the values corresponding to the spin-free  $X^3\Sigma^-$  state.  $R_e$  and  $\omega_e$  for the 2 and  $0^-$  states ( $3.88\text{ a.u.}$  and  $522\text{ cm}^{-1}$ , respectively) almost coincide with the corresponding spin-free  $^3\Pi$  values. For the remaining 1 and  $0^+$  states  $R_e$  and  $\omega_e$  are larger by 0.06 a.u. and  $183\text{--}267\text{ cm}^{-1}$ , respectively. Excitation energies for different SO states lie in the interval of 0.10–0.16 eV. Dissociation energy for the ground  $0^+$  state is 1.54 eV and dissociation energies for different excited SO states (2, 1,  $0^-$ , and  $0^+$ ) are 1.44, 1.41, 1.41 and 1.60 eV, respectively.

### Acknowledgements

The support of the Slovak Research and Development Agency (Contract No. APVV-20-018405) and VEGA (Grant No. 1/3560/06) is acknowledged. The authors acknowledge the support from the Greek Secretariat for research and the Slovak Ministry of Education through a Greece-Slovakia bilateral collaboration program.

### References

- [1] A.G. Bhuiyan, A. Hashimoto, A. Yamamoto, *J. Appl. Phys.* 94 (2003) 2779.
- [2] J. Wu et al., *J. Appl. Phys.* 94 (2003) 4457.
- [3] F.A. Ponce, D.P. Bour, *Nature* 386 (1997) 351.
- [4] W. Walukiewicz et al., *J. Crystal Growth* 269 (2004) 119.
- [5] W. Walukiewicz et al., *J. Phys. D – Appl. Phys.* 39 (2006) R83.
- [6] L.T. Ueno, O. Roberto-Neto, S. Canuto, F.B.C. Machado, *Chem. Phys. Lett.* 413 (2005) 65.
- [7] P.A. Denis, K. Balasubramanian, *Chem. Phys. Lett.* 423 (2006) 247.
- [8] G. Theodorakopoulos, I.D. Petsalakis, *Chem. Phys. Lett.* 423 (2006) 445.
- [9] K. Lawniczak-Jablonska et al., *Phys. Rev. B* 61 (2000) 16623.
- [10] I. Mahboob et al., *Phys. Rev. B* 69 (2004).
- [11] A. Qteish, A.I. Al-Sharif, M. Fuchs, M. Scheffler, S. Boeck, J. Neugebauer, *Comput. Phys. Commun.* 169 (2005) 28.
- [12] A.K. Kandalam, R. Pandey, M.A. Blanco, A. Costales, J.M. Recio, *J. Phys. Chem. B* 104 (2000) 4361.
- [13] A. Costales, A.K. Kandalam, A.M. Pendas, M.A. Blanco, J.M. Recio, R. Pandey, *J. Phys. Chem. B* 104 (2000) 4368.
- [14] R.J. Buenker, S. Krebs, in: K. Hirao (Ed.), *Recent Advances in Multireference Methods*, World Scientific, Singapore, 1999, p. 1.
- [15] J.M.L. Martin, T.J. Lee, G.E. Scuseria, P.R. Taylor, *J. Chem. Phys.* 97 (1992) 6549.
- [16] Y. Mochizuki, K. Tanaka, *Theoret. Chem. Acc.* 101 (1999) 292.
- [17] G.L. Gutsev, P. Jena, R.J. Bartlett, *J. Chem. Phys.* 110 (1999) 2928.
- [18] A. Banerjee, A. Pramanik, K.K. Das, *Chem. Phys. Lett.* 429 (2006) 62.
- [19] L.A. Lajohn, P.A. Christiansen, R.B. Ross, T. Atashroo, W.C. Ermler, *J. Chem. Phys.* 87 (1987) 2812.
- [20] L.F. Pacios, P.A. Christiansen, *J. Chem. Phys.* 82 (1985) 2664.
- [21] B. Roos, R. Lindh, P.-A. Malmqvist, V. Veryazov, P.O. Widmark, *J. Phys. Chem. A* 108 (2004) 2851.
- [22] B.A. Hess, *Phys. Rev. A* 33 (1986) 3742.
- [23] P. Neogrady, M. Urban, I. Hubac, *J. Chem. Phys.* 100 (1994) 3706.
- [24] P. Neogrady, M. Urban, *Int. J. Quantum Chem.* 55 (1995) 187.
- [25] K. Andersson, P.-A. Malmqvist, B. Roos, *J. Chem. Phys.* 96 (1992) 1218.
- [26] G. Karlström et al., *Comput. Mater. Sci.* 28 (2003) 222.
- [27] M. Barysz, A.J. Sadlej, J.G. Snijders, *Int. J. Quantum Chem.* 65 (1997) 225.
- [28] G. Maroulis, *J. Chem. Phys.* 108 (1998) 5432.
- [29] B. Roos, P.-A. Malmqvist, *Phys. Chem. Chem. Phys.* 6 (2004) 2919.